

Light dilution via wavelength management for efficient high-density photobioreactors<sup>†</sup>

Matthew D. Ooms<sup>1</sup>, Percival J. Graham<sup>1</sup>, Brian Nguyen<sup>1</sup>, Edward H. Sargent<sup>2</sup>, David Sinton<sup>1\*</sup>

<sup>1</sup> Department of Mechanical and Industrial Engineering, and Institute for Sustainable Energy,  
University of Toronto, 5 King's College Road, Toronto, M5S 3G8, Canada

<sup>2</sup> Department of Electrical and Computer Engineering, University of Toronto, 10 King's College Rd.  
Toronto, ON. M5S 3G4, Canada

\*Corresponding author: [sinton@mie.utoronto.ca](mailto:sinton@mie.utoronto.ca)

<sup>†</sup>This article has been accepted for publication and undergone full peer review but has not been through the copyediting, typesetting, pagination and proofreading process, which may lead to differences between this version and the Version of Record. Please cite this article as doi: [10.1002/bit.26261]

**This article is protected by copyright. All rights reserved**  
Received December 5, 2016; Revision Received January 24, 2017; Accepted January 30, 2017

## Abstract

The spectral distribution of light influences microalgae productivity; however, development of photobioreactors has proceeded largely without regard to spectral optimization. Here we use monochromatic light to quantify the joint influence of path length, culture density, light intensity and wavelength on productivity and efficiency in *Synechococcus elongatus*. The productivity of green light was ~4 x that of red at the highest levels of culture density, depth and light intensity. This performance is attributed to the combination of increased dilution and penetration of this weakly absorbed wavelength over a larger volume fraction of the reactor. In contrast, red light outperformed other wavelengths in low-density cultures with low light intensities. Low density cultures also adapted more rapidly to reduce absorption of longer wavelengths, allowing for prolonged cultivation. Taken together, these results indicate that, particularly for artificially lit photobioreactors, wavelength needs to be included as a critical operational parameter to maintain optimal performance. This article is protected by copyright. All rights reserved

## 1 Introduction

The productivity of a microalgal cultivation operation determines its profitability. Ideally, high productivity is paired with high-efficiency conversion of light into bio-products, though this is rarely achieved (Goldman, 1979). High productivity requires high intensity light, and this typically has a negative impact on photosynthetic efficiency owing to energy losses that occur when the light intensity nears or exceeds the saturation limit of the organism (Goldman, 1979; Simionato et al., 2013). Full sunlight can be many times greater than this saturation limit, necessitating strategies to reduce photoinhibition and increase photosynthetic efficiency without compromising productivity (Ooms et al., 2016). Large scale photobioreactor design requires optimizing the combination of culture depth, optical density, and mixing rate in order to maintain an optimal light environment inside the photobioreactor (Cuaresma et al., 2009; Dye et al., 2011; Pierobon et al., 2014; Posten, 2009). Genetic engineering of microalgae to reduce the light harvesting antenna size has also been explored as a means of reducing the cell's absorption and allowing it to tolerate higher light intensities (Kirst et al., 2014; Kwon et al., 2013; de Mooij et al., 2015; Ort and Melis, 2011).

Modifying the spectral quality of light also presents an opportunity to dilute light to compatible intensities by managing its wavelength, as described in Fig. 1a. Particularly with increasing use of light emitting diodes (LEDs), the question of spectral dependency of light penetration is becoming more important for both lab scale studies and commercial applications (Schulze et al., 2014). The effects of light quality on growth and morphology have been reviewed, (Wang et al., 2014) generally showing that red light is more effective for growth, due to improved absorption by light harvesting pigments such as chlorophyll. (Baer et al., 2016; Markou, 2014; Mattos et al., 2015; de Mooij et al., 2016; Ra et al., 2016; Schulze et al., 2014; Wang et al., 2007). For example *Chlamydomonas reinhardtii* grown under moderate light intensity ( $100 \mu\text{mol}_{\text{photons}}/\text{m}^2 \cdot \text{s}$ ) and low culture density showed

peak productivity when primarily red light was used, compared to green and blue (Baer et al., 2016).

In another study which used high intensity light ( $1500 \mu\text{mol}_{\text{photons}}/\text{m}^2\cdot\text{s}$ ) a culture density of  $2.96 \text{ g}_{\text{dry}}/\text{L}$

● *C. reinhardtii* performed best when yellow light was used (de Mooij et al., 2016). Green alga

*Scenedesmus bijuga* had the highest efficiency based on evolved oxygen under green light at relatively high light intensity ( $500 \mu\text{mol}_{\text{photons}}/\text{m}^2\cdot\text{s}$ ) and high culture density  $> 2 \text{ g}_{\text{dry}}/\text{L}$  (Mattos et al., 2015). In

contrast, cultures of the cyanobacteria *Spirulina platensis* performed best under red light at high light intensity ( $3000 \mu\text{mol}_{\text{photons}}/\text{m}^2\cdot\text{s}$ ) and for low culture density ( $\text{OD} < \sim 1$ ) (Wang et al., 2007). The

particular suite and relative concentration of photosynthetic pigments present in an organism also leads to species dependent variation – cyanobacteria in particular are often equipped with phytochromes

which are sensitive to short-wavelength light and can trigger photo-protection mechanisms (Bailey and Grossman, 2008; El Bissati et al., 2000; Kirilovsky, 2007). With respect to frequency, it has been well

documented that the frequency and duty cycle of pulsed light can significantly alter the productivity of microalgae (Matthijs et al., 1996; Vejrazka et al., 2013). Collectively, these past results are difficult to

reconcile due to the coupled influence on productivity of culture density, light intensity, path length, frequency and species differences.

In this work, we quantify the effects of spectral quality and light dilution on photosynthetic efficiency and productivity in cultures of *Synechococcus elongatus* under high and low light intensity, high and low initial culture density, and long and short culture depths. Cultures were grown in lab-scaled column reactors with reflective sidewalls coupled to monochromatic light emitting diodes of five different wavelengths. Each light source was equipped with collimating optics to simulate direct beam radiation. Four different sets of conditions were explored, including two different initial culture densities for two different culture depths. These combinations were repeated for both low ( $50 \mu\text{mol}_{\text{photons}}/(\text{m}^2\cdot\text{s})$ ) and high  $2000 \mu\text{mol}_{\text{photons}}/(\text{m}^2\cdot\text{s})$  light intensities for a total of eight scenarios.

Commonly used red light is indeed found to perform well at low density and low intensity. This trend

is reversed, however, when the culture conditions are changed to high intensity and high density, with weakly absorbed green light significantly outperforming other wavelengths. Furthermore, significant changes in cell pigmentation were observed for longer wavelength light as cells adapted to their new light environment.

## 2 Materials and methods

### 2.1 Cyanobacteria cultures

Cultures of kanamycin resistant *Synechococcus elongatus* T2SE provided by professor Rakefet Schwarz of Bar-Ilan University, Israel, were cultured under  $30 \mu\text{mol}_{\text{photons}}/(\text{m}^2 \cdot \text{s})$  warm white fluorescent illumination with constant agitation, at  $30^\circ\text{C}$  (Schatz et al., 2013). Cells were kept in exponential growth phase through periodic dilution with fresh media. HEPES buffered (pH 8) 2x BG11 media (Sigma Aldrich, 73816) supplemented with 50 mg/L kanamycin was used for all experiments and culture maintenance to ensure cells were not nutrient limited. Cells were centrifuged and re-suspended in fresh media to the required density prior to experiments.

### 2.2 Monochromatic LED photobioreactors

Monochromatic LED photobioreactors, shown schematically in Fig. 1b, were constructed from 1” diameter acrylic tubing. The reactors were liquid and gas tight, except for a tube used to bubble in 5% CO<sub>2</sub> in air. The exterior of each reactor was clad with a smooth layer of aluminum foil to reflect light incident on the sidewall back towards the culture. A fused silica glass window mounted inside a 1” aluminum lens tube (Thorlabs, SM1L03) was mounted to the bottom of the tube which both sealed the base of the reactor and provided a convenient interface with the illumination system. The reactors were operated with culture volumes of 10 mL and 30 mL resulting in culture depths of 2 cm and 6 cm respectively. The tops of the reactors were sealed with an acrylic cap including a port for a 3-mm diameter aeration tube. A constant flow of 5% CO<sub>2</sub> in air was filtered and humidified before being bubbled into each reactor at a rate of  $\sim 1.5 \text{ m}^3/\text{hr}$ . CO<sub>2</sub> concentration was monitored with an inline CO<sub>2</sub>

meter (CO2Meter, CM-0123). Evaporation losses were monitored by measuring the mass of each reactor daily and replacing the difference with deionized water. Daily evaporative losses were typically less than ~1% of total volume.

For all experiments, light was supplied from below using high power LEDs controlled with a custom made constant-current power supply. Five different wavelengths were tested, with center wavelengths at 454 nm, 534 nm, 593 nm, 630 nm, and 660 nm. Normalized emission spectra for the LEDs are shown in Fig. 1c, measured with a fiber coupled spectrometer (Ocean Optics USB2000+). Light from the LEDs was collimated and directed into the photobioreactor using an aspheric condenser lens (Thorlabs ACL25416U) to mimic the direct collimated radiation received by outdoor photobioreactors from the sun. The intensity of each LED was monitored using a photodiode power sensor calibrated at each respective wavelength, and was set to  $50 \mu\text{mol}_{\text{photons}}/(\text{m}^2 \cdot \text{s})$  for low light experiments and  $2000 \mu\text{mol}_{\text{photons}}/(\text{m}^2 \cdot \text{s})$  for high light experiments.

During each experiment, three photobioreactors of each wavelength were operated inside a temperature controlled enclosure maintained at 30°C. Here, 30°C was chosen as a representative temperature for photobioreactor operation, and to be between the upper and lower temperature thresholds for sustained growth in this organism (Krüger and Eloff, 1978). Each LED was mounted onto an aluminum heat-sink to prevent direct heating of the culture by the LED. During high-light experiments, additional heat transfer away from the LEDs was achieved through forced convection with fans, ensuring culture temperatures were maintained at  $30^\circ\text{C} \pm 0.5^\circ\text{C}$ . At lower light intensities, forced convection cooling was not required.

### **2.3 Biomass growth estimation and attenuation spectra**

Attenuation spectra and optical density were measured using a halogen light source and spectrometer (Ocean Optics USB2000+) coupled to a 10 mm cuvette holder. Biomass accumulation

was estimated from these spectra by first determining the optical density of the suspension at a wavelength of 750 nm ( $OD_{750}$ ). Prior to each measurement, samples were withdrawn from each photobioreactor and diluted below  $OD_{750_{10mm}} = 1.0$ . We verified that biomass was proportional to optical density, for the range of densities measured, by performing dry mass measurements of cell suspensions of various densities (Moheimani et al., 2013). For reference, an optical density of 1 (corresponding to a 10 mm cuvette) corresponded to a dry mass of 0.28 g/L.

## 2.4 Photobioreactor photon conversion efficiency (PCE)

We define the photon conversion efficiency as the energy efficiency of converting incident light to stored biomass, according to:

$$PCE_{\lambda} = \frac{P_{\lambda} \cdot G_{biomass}}{\frac{h \cdot c}{\lambda} \cdot I_{PPFD}}$$

Where  $P_{\lambda}$  is the areal productivity of the culture at a given wavelength,  $G_{biomass}$  the biomass energy content,  $h$  is Planck's constant,  $c$  is the speed of light,  $\lambda$  is the wavelength of light, and  $I_{PPFD}$  is the quantum intensity of light. The value for biomass energy content used in this study was approximated from literature to be 21 kJ/g<sub>dw</sub>. (Goldman, 1979; Taylor et al., 1988; Weyer et al., 2010) While this is not an exact value, it is a useful approximation for obtaining a reasonable estimate of photobioreactor efficiency.

The maximum theoretical productivity for outdoor microalgal photosynthesis has been estimated to be ~8-12% based on full spectrum sunlight (Bolton and Hall, 1991; Melis, 2009; Weyer et al., 2010; Zhu et al., 2008). These values account for the ~57% of sunlight which falls outside the visible spectrum and is of little use for photosynthesis (Weyer et al., 2010), and for losses internal to the photosynthetic energy conversion process. These internal losses are related to the quantum

requirement of CO<sub>2</sub> fixation which is the number of photons required to fix one CO<sub>2</sub> molecule as described in the simplified photosynthesis equation:



Estimates for the quantum requirement range between 6 and 13, with consensus suggesting 8 as a reasonable middle ground (Bolton and Hall, 1991). The product of photosynthesis, CH<sub>2</sub>O represents the simplest form of carbohydrate and the starting point from which more complex molecules are assimilated. The equation for the efficiency of photosynthesis ( $\epsilon_{\text{internal}}$ ) is simply the ratio of the energy contained in this product ( $E_{\text{CH}_2\text{O}}$ ) relative to the energy of absorbed photons ( $E_{\text{photons}}$ ), which is wavelength dependent:

$$\epsilon_{\text{internal}} = \frac{E_{\text{CH}_2\text{O}}}{8 * E_{\text{photons}}}$$

Since effectively all the light emitted from a monochromatic LED is in the visible range and is therefore useful for photosynthesis, the maximum photon conversion efficiency can be calculated directly from this equation and is ~22% for 454-nm blue light up to 33% for 660-nm red light, assuming the energy content of CH<sub>2</sub>O to be 483 kJ/mol (Weyer et al., 2010). For full spectrum sunlight, an additional factor of 43% accounts for the photosynthetically active portion of the spectrum and leads to sun-lit maximum efficiencies of ~12%. Comparing photon conversion efficiencies between sun-lit cultures and LED-lit cultures must therefore consider the difference in illumination spectrum, as above.



### **3 Results and Discussion**

#### **3.1 Photic zone - light intensity variation within the culture**

As the biomass density in a culture increases, inter-cell shading results in attenuation of light in the direction of propagation leading to heterogeneous light intensity in the reactor, and is different for each wavelength of light as seen in Fig. 2a-b. This attenuation is commonly approximated using the Beer-Lambert law which describes a simple exponential decay of light due to absorption. The Beer-Lambert law however presupposes a non-scattering media which, for microalgal suspensions, is only approximated when the culture density is very low. Alternatively, Cornet's model of one-dimensional transfer using Schuster's approximation is a solution to the radiative transfer equation applicable for photobioreactor architectures where light is propagating and is scattered along a single axis in both forward and backward directions (Cornet et al., 1992a; Cornet et al., 1992b). Simplifying the radiative transfer equations to a single axis allows for analytical expressions for the intensity of the light with respect to depth to be derived. Cornet's model requires the absorption and scattering cross-section spectra of the cells to be known in advance. Here, approximations based on the measured attenuation spectra of *S. elongatus* and the scattering profile described by Stramski have been used. (Stramski et al., 1995; Stramski and Mobley, 1997). Figure 2c compares the results of this model against direct measurements of light transmission for an optical density of  $OD_{750,10\text{mm}} = 0.5$ , matching closely with Cornet's model and highlighting the inadequacy of the Beer-lambert equation in scattering cultures. Using this model, the volume fraction of the culture exposed to actinic light can be approximated for each scenario explored in this study, as shown in Fig. 2d-e.

#### **3.2 Low light – effects of path length and culture density**

For the case of low light intensity, four sets of conditions were used to study the combined effects of path length, culture density, and wavelength. For each wavelength, both short (2 cm, requiring a 10 mL volume) and long (6 cm, requiring a 30 mL volume) culture depths were tested with both low (0.04

This article is protected by copyright. All rights reserved

g/L) and high (0.58 g/L) initial culture densities. It is noteworthy that culture densities in microalgal operations frequently exceed 0.58 g/L (Eustance et al., 2015; Gamage et al., 2011; de Marchin et al., 2015; Masojídek et al., 2011). A moderate high-density level was selected as it was approximately an order of magnitude greater than the low density condition, and captures the inherent effects of dense cultures (exacerbated further at increased densities). Fig. 3 shows the productivity and photon conversion efficiency of cultures cultivated under these four conditions with low light intensity. In all cases here, the culture was light limited. The efficiency is high since the entire culture was well below the saturating intensity.

Fig. 3 shows the productivity for all reactor cases at low light. At high initial culture density (Fig. 3a-b), light gradients resulted in light and dark zones within the reactor volume (Fig. 2d) with cells continually cycling between them. Because of the high initial culture density, virtually all the light of each wavelength was absorbed. The resulting productivity was similar in magnitude in both short and long light-path reactors with high initial culture density, with the exception of 593-nm orange and 630-nm red light which were less productive in the deeper reactor. This reduction was likely related to the frequency at which cells cycled through the illuminated portion of the reactor, and the relative size of that photic zone (which is different for each wavelength, Fig. 2). With respect to the size of the photic zone, the photic zone in the 534-nm green light reactor was 1.3-fold longer than that of the 630-nm red light reactor with high culture depth.

For low-light cases with low initial culture density, Fig. 3c-d, the effects of light gradients were minimized and unabsorbed light which passed through the culture became an increasingly important factor affecting productivity. In both short and long light-path reactors, weakly absorbed green light showed significantly lower productivity than longer wavelengths, since more of the light was able to pass through the reactor and lost. Indeed, the productivity and photon conversion efficiency of all wavelengths in the long light-path reactors (Fig. 3d) improved over the short light-path reactors due to

increased absorption in the deeper culture, with green light showing a 128% increase in productivity and a 2.3-fold increase in photon conversion efficiency. Despite this improvement, for low-density low-light cases, longer wavelengths (593-nm orange, 630-nm red and 660-nm red) outperformed 534-nm green light. The highest productivity and photon conversion efficiency resulted from 630-nm red light due to more complete absorption of light at sub-saturating intensities. These low-density results are in line with previous observations which suggest that red is most effective for microalgal cultivation at low culture density (Baer et al., 2016; Wang et al., 2007).

In all cases, 454-nm blue light underperformed compared with other wavelengths at the same intensity. Due to their complement of pigments, cyanobacteria are known to respond poorly to shorter-wavelength light (Chen et al., 2010; Graham et al., 2015; Itoh et al., 2014). In spite of the strong absorption of blue light at 454 nm, a large portion of the energy is diverted to other pathways (Bailey and Grossman, 2008). Specifically, non-photochemical quenching of absorbed light energy in cyanobacteria is typically induced through a series of reconfigurations triggered by blue-light absorbing proteins (Bailey and Grossman, 2008). The poor productivity from monochromatic blue light are therefore an anomaly among the wavelengths tested here – triggering photo-protection mechanisms not triggered by other wavelengths (Bailey and Grossman, 2008; El Bissati et al., 2000; Kirilovsky, 2007).

Table 1 lists the highest areal productivity and photon conversion efficiency achieved for each wavelength under low light conditions (and corresponding volumetric productivity). Collectively, these low-light condition results indicate that for low culture densities, red light is the preferred wavelength to maximize productivity and efficiency. Increasing culture density increases the effects of light gradients on culture performance which are also wavelength dependent. With highly absorbed wavelengths in dense cultures, a large portion of the reactor volume becomes dark resulting in a larger penalty for 630-nm red light in particular. The ability for green light to penetrate deeper into high-density cultures compared to other wavelengths makes it competitive with other wavelengths at higher

culture density. It is worth noting that the maximum areal productivity does not necessarily correspond to the maximum volumetric productivity – a metric commonly used in photobioreactor analysis. As table 1 shows, 630-nm red light achieved the highest areal productivity even though the 593-nm orange light resulted in a higher volumetric productivity under low light. This is entirely related to the difference in reactor volumes. Peak areal productivity under 630-nm light occurred in reactors with long light paths (i.e. larger volume), compared to 593-nm light which performed best with short light paths. As a result, the volumetric productivity was lower in the larger volume reactors even though those reactors generated more biomass in total. Here, because the objective is to achieve maximum light utilization, results were evaluated based on areal productivity.

### **3.3 High light – effects of path length and culture density**

When the light intensity was increased far above the saturation limit of the cells, the trends observed in the low light trials no longer applied, as is evident in Fig. 4. Notably, 534-nm green light demonstrated the highest productivity and efficiency under high light conditions in all cases, with 630-nm red light generally showing much lower performance.

For low-density cultures the trend of performance across the spectrum in high-light (Fig. 4c-d) was a reversal of that observed for low-light (Fig. 3c-d). In these cases, and especially those with short culture depth, the whole reactor volume was in the photic zone (Fig. 2e), and thus no dark zone was present. The observed wavelength dependence on productivity in low density cultures is attributed here to increased resilience of the culture to weakly absorbed light. Specifically, green outperformed red 2:1 at high light intensity, chiefly because less light was absorbed per cell and the effects of photoinhibition were mitigated since the light was weakly absorbed.

At high culture densities, cell shading (photic zone) played a role in productivity. The photic zone for green light is ~ 1.6-fold that of red light (Fig. 2e), resulting in a larger relative fraction of productive

culture volume. This larger volume for green light resulted in a ~ 4-fold increase in green light performance over red (at the highest levels of culture density, culture depth and light intensity).

The wavelength dependence on photon conversion efficiency correlates directly with areal productivity and thus showed the same general trends discussed above. Because photon conversion efficiency takes into account the energy content of photons, there is an efficiency penalty for shorter wavelengths such as green light. In spite of this penalty, green light outperformed the other wavelengths in terms of *both* productivity and efficiency at high light conditions. In terms of photon conversion efficiency alone, low-light cases outperformed high-light dramatically (~ an order of magnitude, from 10% to 1%), illustrating the tradeoff between productivity and efficiency in operations.

While the spectral performance between high and low light scenarios was remarkably different, the relative performance between low- and high-density, and short and long light path scenarios was similar. In particular, for high density cultures, transitioning from a short to long path length (Fig. 4a-b) resulted in a decrease in productivity and photosynthetic efficiency owing to an increase in the ratio of dark to light volume in the reactor. In addition, for low density cultures, transitioning from a short to long path length (Fig. 4c-d) resulted in increased productivity and efficiency, owing to more complete absorption of the available photons.

Table 1 highlights the maximum productivity and efficiency achieved for each wavelength under high light. Green light achieved the highest areal productivity, outperforming 454-nm blue 4.1-fold, 593-nm orange by 1.5-fold, 630-nm red by 2.2-fold and 660-nm red by 1.6-fold. For all wavelengths, peak productivity was achieved with high light, high density, and short path length. Peak efficiency was achieved for all wavelengths with low light. For 454-nm, 630-nm and 660-nm light, peak efficiency was achieved with low density and long path length. For 534-nm and 593-nm light, peak

efficiency was achieved with high density and short path length. In spite of the lack of light harvesting pigments with absorption peaks in the green region, the high performance of the cultures under high intensity green light indicates that absorbed green photons can be as productive as absorbed photons of other colors. The high performance of green light is attributed to the spatial dilution achieved due to weakly absorbed light.

### **3.4 Batch cultivation**

The reactors were operated in batch mode for four days. The accumulated biomass relative to each experiment's starting condition is plotted in Fig. 5. Accumulated biomass is reported in Fig. 5 to illustrate the efficacy of each reactor scenario at generating biomass under a given light intensity. This result is masked for different reactor depths if the volume normalized biomass concentration is instead used. To determine the cell concentration, the accumulated biomass can be divided by reactor volume (10 mL for the shallow reactors and 30 mL for the deep reactors). Low light experiments demonstrated consistent growth over the duration of the experiment. Under high light conditions however, growth rates slowed and for several cases became negative after ~3 days. This decline was most notable for longer wavelengths (593 nm, 630 nm, and 660 nm) and least pronounced for 534-nm green light. The most likely cause for the reduction in productivity and loss of biomass relates to accumulated photo-damage at high irradiance, particularly for the highly absorbed wavelengths.

Significant changes in cell pigmentation also occurred for 593-nm, 630-nm, and 660-nm light at high intensity, as shown in Fig. 6, and are indicative of chromatic adaptation in response to the high light conditions. Changes in pigmentation in response to light are common in macroalgae and cyanobacteria (Forest, 2014; Katsuda et al., 2004; Korbee et al., 2005; Schulze et al., 2014), and can result from light induced damage (photobleaching) (Miller, 1991) or as a physiological response (Gutu and Kehoe, 2012; Palenik, 2001; Tandeau de Marsac, 1977). For instance, chromatic adaptation in cyanobacteria allows for the customization of light harvesting pigment composition and expression

within the cell in response to changing light intensity and quality (Gutu and Kehoe, 2012; Kulkarni and Golden, 1994; Shukla et al., 2012). While indication of pigmentation change was evident in all high light scenarios, for cultures that began with high cell density (Fig. 5(e-f)) the adaptation response appeared to be slower. For these cultures, the biomass concentration plateaued early, after ~3 days (Fig. 5e-f), and in many cases began to decrease, with only a moderate shift in the pigmentation of the cells (Fig. 6a-b). This trend contrasts with that observed for cultures that began with low initial cell densities (Fig. 5g-h) for which an obvious adaptation in cell color and attenuation spectrum occurred (Fig. 6c-d). Notably, this shift in pigmentation was accompanied by a much smaller decrease in culture density (Fig. 5g-h) compared to the high initial culture density reactors, suggesting that the deleterious effects of high light intensity over time were in part mitigated by the more rapid shift in pigment content. In summary, a low initial culture density allowed more cells to be exposed to high light conditions early, inducing more rapid adaptation and less damage.

#### 4 Conclusions

To maximize the cost effectiveness of microalgae cultivation, productivity and efficiency must be maximized (Stephens et al., 2010). Here we demonstrated that contrary to conventional wisdom, highly absorbed red light is not necessarily the wavelength of choice for monochromatic cultivation, particularly for high density cultures typical of industrial operations. Instead, depending on culture density, depth and irradiance, weakly absorbed green light may provide the best option for achieving high productivity with increased efficiency because it is able to dilute the light over a larger portion of the reactor.

#### 5 Acknowledgements

This work was supported through a Strategic Grant from the Natural Science and Engineering Research Council of Canada, the University of Toronto Connaught Global Scholars Program in Bio-

Inspired Ideas for Sustainable Energy, the University of Toronto McLean Senior Fellowship (DS), and the Vanier Canada Graduate Scholarship (MO). PG gratefully acknowledges NSERC PGS and Hatch Scholarships. BN gratefully acknowledges funding from Ontario Graduate Scholarships, the Queen Elizabeth II Graduate Scholarships in Science & Technology, NSERC CGS Scholarships and the MEET, NSERC CREATE Program.

## 6 Conflicts of Interest

The authors have no conflicts of interest to declare.

## 7 References

- Baer S, Heining M, Schwerna P, Buchholz R, Hübner H. 2016. Optimization of spectral light quality for growth and product formation in different microalgae using a continuous photobioreactor. *Algal Res.* **14**:109–115.
- Bailey S, Grossman A. 2008. Photoprotection in cyanobacteria: Regulation of light harvesting. *Photochem. Photobiol.* **84**:1410–1420.
- El Bissati K, Delphin E, Murata N, Etienne A-L, Kirilovsky D. 2000. Photosystem II fluorescence quenching in the cyanobacterium *Synechocystis* PCC 6803: involvement of two different mechanisms. *Biochim. Biophys. Acta - Bioenerg.* **1457**:229–242.
- Bolton JR, Hall DO. 1991. The Maximum Efficiency of Photosynthesis. *Photochem. Photobiol.* **53**:545–548.
- Chen HB, Wu JY, Wang CF, Fu CC, Shieh CJ, Chen CI, Wang CY, Liu YC. 2010. Modeling on chlorophyll a and phycocyanin production by *Spirulina platensis* under various light-emitting diodes. *Biochem. Eng. J.* **53**:52–56.
- Cornet JF, Dussap CG, Dubertret G. 1992a. A structured model for simulation of cultures of the cyanobacterium *Spirulina platensis* in photobioreactors: I. Coupling between light transfer and growth kinetics. *Biotechnol. Bioeng.* **40**:817–825.
- Cornet JF, Dussap CG, Cluzel P, Dubertret G. 1992b. A structured model for simulation of cultures of the cyanobacterium *Spirulina platensis* in photobioreactors: II. Identification of kinetic parameters under light and mineral limitations. *Biotechnol. Bioeng.* **40**:826–834.
- Cuaresma M, Janssen M, Vélchez C, Wijffels RH. 2009. Productivity of *Chlorella sorokiniana* in a short light-path (SLP) panel photobioreactor under high irradiance. *Biotechnol. Bioeng.* **104**:352–359.
- Dye D, Muhs J, Wood B, Sims R. 2011. Design and Performance of a Solar Photobioreactor Utilizing Spatial Light Dilution. *J. Sol. Energy Eng.* **133**:15001.
- Eustance E, Badvipour S, Wray JT, Sommerfeld MR. 2015. Biomass productivity of two *Scenedesmus* strains cultivated semi-continuously in outdoor raceway ponds and flat-panel photobioreactors. *J. Appl. Phycol.*



- Forest KT. 2014. Vivid watercolor paintbox for eukaryotic algae. *Proc. Natl. Acad. Sci.* **111**:5448–5449.
- Gamage AM, Shui G, Wenk MR, Chua KL. 2011. N-Octanoylhomoserine lactone signalling mediated by the BpsI-BpsR quorum sensing system plays a major role in biofilm formation of *Burkholderia pseudomallei*. *Microbiology* **157**:1176.
- Goldman JC. 1979. Outdoor algal mass cultures. II. Photosynthetic yield limitations. *Water Res.* **13**:119–136.
- Graham PJ, Riordon J, Sinton D. 2015. Microalgae on display: a microfluidic pixel-based irradiance assay for photosynthetic growth. *Lab Chip* **15**:3116–3124.  
<http://xlink.rsc.org/?DOI=C5LC00527B>.
- Gutu A, Kehoe DM. 2012. Emerging perspectives on the mechanisms, regulation, and distribution of light color acclimation in cyanobacteria. *Mol. Plant* **5**:1–13.  
<http://www.ncbi.nlm.nih.gov/pubmed/21772031>.
- Itoh KI, Nakamura K, Aoyama T, Kakimoto T, Murakami M, Takido T. 2014. The influence of wavelength of light on cyanobacterial asymmetric reduction of ketone. *Tetrahedron Lett.* **55**:435–437.
- Katsuda T, Lababpour A, Shimahara K, Katoh S. 2004. Astaxanthin production by *Haematococcus pluvialis* under illumination with LEDs. *Enzyme Microb. Technol.* **35**:81–86.
- Kirilovsky D. 2007. Photoprotection in cyanobacteria: the orange carotenoid protein (OCP)-related non-photochemical-quenching mechanism. *Photosynth. Res.* **93**:7–16.  
<http://www.springerlink.com/index/10.1007/s11120-007-9168-y>.
- Kirst H, Formighieri C, Melis A. 2014. Maximizing photosynthetic efficiency and culture productivity in cyanobacteria upon minimizing the phycobilisome light-harvesting antenna size. *Biochim. Biophys. Acta - Bioenerg.* **1837**:1653–1664.
- Korbee N, Figueroa FL, Aguilera J. 2005. Effect of light quality on the accumulation of photosynthetic pigments, proteins and mycosporine-like amino acids in the red alga *Porphyra leucosticta* (Bangiales, Rhodophyta). *J. Photochem. Photobiol. B Biol.* **80**:71–78.
- Krüger GHJ, Eloff JN. 1978. the Effect of Temperature on Specific Growth Rate and Activation Energy of *Microcystis* and *Synechococcus* Isolates Relevant To the Onset of Natural Blooms. *J. Limnol. Soc. South. Africa* **4**:9–20.
- Kulkarni RD, Golden SS. 1994. Adaptation to high light intensity in *Synechococcus* sp. strain PCC 7942: regulation of three *psbA* genes and two forms of the D1 protein. *J. Bacteriol.* **176**:959.
- Kwon JH, Bernát G, Wagner H, Rögner M, Rexroth S. 2013. Reduced light-harvesting antenna: Consequences on cyanobacterial metabolism and photosynthetic productivity. *Algal Res.* **2**:188–195.
- de Marchin T, Erpicum M, Franck F. 2015. Photosynthesis of *Scenedesmus obliquus* in outdoor open thin-layer cascade system in high and low CO<sub>2</sub> in Belgium. *J. Biotechnol.* **215**:2–12.
- Markou G. 2014. Effect of various colors of light-emitting diodes (LEDs) on the biomass composition of *Arthrospira platensis* cultivated in semi-continuous mode. *Appl. Biochem. Biotechnol.* **172**:2758–2768.
- Masojídek J, Kopecký J, Giannelli L, Torzillo G. 2011. Productivity correlated to photobiochemical performance of *Chlorella* mass cultures grown outdoors in thin-layer cascades. *J. Ind. Microbiol. Biotechnol.* **38**:307–317.

- Matthijs HCP, Balke H, Van Hes UM, Kroon BM a, Mur LR, Binot R a. 1996. Application of light-emitting diodes in bioreactors: Flashing light effects and energy economy in algal culture (*Chlorella pyrenoidosa*). *Biotechnol. Bioeng.* **50**:98–107.
- Mattos ER, Singh M, Cabrera ML, Das KC. 2015. Enhancement of biomass production in *Scenedesmus bijuga* high-density culture using weakly absorbed green light. *Biomass and Bioenergy* **81**:473–478.
- Melis A. 2009. Solar energy conversion efficiencies in photosynthesis: Minimizing the chlorophyll antennae to maximize efficiency. *Plant Sci.* **177**:272–280.  
<http://linkinghub.elsevier.com/retrieve/pii/S0168945209001861>.
- Miller N. 1991. Energy dissipation and photoprotection mechanisms during chlorophyll photobleaching in thylakoid membranes. *Photochem. Photobiol.* **54**:465–472.
- Moheimani NR, Borowitzka MA, Isdepsy A, Sing SF. 2013. Standard Methods for Measuring Growth of Algae and Their Composition. In: . *Algae for Biofuels and Energy*. Dordrecht: Springer Netherlands, pp. 265–284.
- de Mooij T, Janssen M, Cerezo-Chinarro O, Mussnug JH, Kruse O, Ballottari M, Bassi R, Bujaldon S, Wollman F-A, Wijffels RH. 2015. Antenna size reduction as a strategy to increase biomass productivity: a great potential not yet realized. *J. Appl. Phycol.* **27**:1063–1077.
- de Mooij T, de Vries G, Latsos C, Wijffels RH, Janssen M. 2016. Impact of light color on photobioreactor productivity. *Algal* **15**:32–42.
- Ooms MD, Dinh CT, Sargent EH, Sinton D. 2016. Photon management for augmented photosynthesis. *Nat. Commun.* **7**:12699.
- Ort DR, Melis A. 2011. Optimizing antenna size to maximize photosynthetic efficiency. *Plant Physiol.* **155**:79–85.
- Palenik B. 2001. Chromatic Adaptation in Marine Synechococcus Strains **67**:991–994.
- Pierobon SC, Ooms MD, Sinton D. 2014. Evanescent cultivation of photosynthetic bacteria on thin waveguides. *J. Micromechanics Microengineering* **24**:45017. <http://stacks.iop.org/0960-1317/24/i=4/a=045017?key=crossref.8af4d4e2c5bbb544dcf2f02e6b1a333b>.
- Posten C. 2009. Design principles of photo-bioreactors for cultivation of microalgae. *Eng. Life Sci.* **9**:165–177.
- Ra CH, Kang CH, Jung JH, Jeong GT, Kim SK. 2016. Effects of light-emitting diodes (LEDs) on the accumulation of lipid content using a two-phase culture process with three microalgae. *Bioresour. Technol.* **212**:254–261. <http://dx.doi.org/10.1016/j.biortech.2016.04.059>.
- Schatz D, Nagar E, Sendersky E, Parnasa R, Zilberman S, Carmeli S, Mastai Y, Shimoni E, Klein E, Yeger O, Reich Z, Schwarz R. 2013. Self-suppression of biofilm formation in the cyanobacterium *Synechococcus elongatus*. *Environ. Microbiol.* **15**:1786–1794.  
<http://www.ncbi.nlm.nih.gov/pubmed/23298171>.
- Schulze PSC, Barreira L a., Pereira HGC, Perales J a., Varela JCS. 2014. Light emitting diodes (LEDs) applied to microalgal production. *Trends Biotechnol.*:1–9.  
<http://linkinghub.elsevier.com/retrieve/pii/S0167779914001115>.
- Shukla A, Biswas A, Blot N, Partensky F, Karty J a, Hammad L a, Garczarek L, Gutu A, Schluchter WM, Kehoe DM. 2012. Phycoerythrin-specific bilin lyase-isomerase controls blue-green chromatic acclimation in marine *Synechococcus*. *Proc. Natl. Acad. Sci. U. S. A.* **109**:20136–41.

- Simionato D, Basso S, Giacometti GM, Morosinotto T. 2013. Optimization of light use efficiency for biofuel production in algae. *Biophys. Chem.* **182**:71–78. <http://www.ncbi.nlm.nih.gov/pubmed/23876487>.
- Stephens E, Ross IL, Mussgnug JH, Wagner LD, Borowitzka M a., Posten C, Kruse O, Hankamer B. 2010. Future prospects of microalgal biofuel production systems. *Trends Plant Sci.* **15**:554–564.
- Stramski D, Mobley CD. 1997. Effects of microbial particles on oceanic optics: A database of single-particle optical properties. *Limnol. Oceanogr.* **42**:538–549.
- Stramski D, Shalapyonok A, Reynolds RA. 1995. Optical characterization of the oceanic unicellular cyanobacterium *Synechococcus* grown under a day-night cycle in natural irradiance. *J. Geophys. Res.* **100**:13295.
- Tandeau de Marsac N. 1977. Occurrence and nature of chromatic adaptation in cyanobacteria. *J. Bacteriol.* **130**:82–91.
- Taylor P, Tredici MR, Margheri MC, De Philippis R, Bocci F, Materassi R. 1988. Marine Cyanobacteria as a Potential Source of Biomass and Chemicals. *Int. J. Sustain. Energy* **6**:235–246.
- Vejrazka C, Janssen M, Benvenuti G, Streefland M, Wijffels RH. 2013. Photosynthetic efficiency and oxygen evolution of *Chlamydomonas reinhardtii* under continuous and flashing light. *Appl. Microbiol. Biotechnol.* **97**:1523–32. <http://www.ncbi.nlm.nih.gov/pubmed/23001055>.
- Wang CY, Fu CC, Liu YC. 2007. Effects of using light-emitting diodes on the cultivation of *Spirulina platensis*. *Biochem. Eng. J.* **37**:21–25.
- Wang S-K, Stiles AR, Guo C, Liu C-Z. 2014. Microalgae cultivation in photobioreactors: An overview of light characteristics. *Eng. Life Sci.*:n/a-n/a. <http://doi.wiley.com/10.1002/elsc.201300170>.
- Weyer KM, Bush DR, Darzins A, Willson BD. 2010. Theoretical maximum algal oil production. *Bioenergy Res.* **3**:204–213.
- Zhu XG, Long SP, Ort DR. 2008. What is the maximum efficiency with which photosynthesis can convert solar energy into biomass? *Curr. Opin. Biotechnol.* **19**:153–159.

**Table 1: Light quality effects on productivity and photon conversion efficiency**

Wavelength [nm]	Low Light		Volumetric Prod. [g/(L·day)]	High Light		Volumetric Prod. [g/(L·day)]
	Max Areal Prod. [g/(m <sup>2</sup> ·day)]	PCE [%]		Max Areal Prod. [g/(m <sup>2</sup> ·day)]	PCE [%]	
454	0.9	1.7	0.01	6.8	0.3	0.28
534	3.7	8.0	0.05	28	1.5	1.17
593	3.7	9.0	0.15	19	1.1	0.78
630	4.3	11	0.06	13	0.8	0.55
660	3.9	10.5	0.05	18	1.2	0.75

## Figures:

Fig. 1. Light wavelength effects on light harvesting and photobioreactor design. (i) When light is incident upon a microalgal culture, the rate of absorption is determined by the particular light harvesting pigments contained in the cell and define its (ii) absorption cross section. At equal photon fluxes, a smaller absorption cross section results in fewer absorbed photons per cell. Selecting a weakly absorbed wavelength can cause the photon absorption rate per cell to be below the saturation limit, resulting in greater efficiency per cell, but lower productivity compared to a strongly absorbed wavelength. (iv) The reduced productivity per cell that results from low absorption can be offset by raising the number of cells either by increasing the reactor depth and/or increasing the culture density. (b) Schematic of the photobioreactors used in this study showing light from an LED emitter being collimated into the reactor vessel to achieve uniform, direct irradiation. (c) The measured emission spectra of the light emitting diodes used and the measured attenuation spectra of *S. elongatus*.

Fig. 2. Attenuation of light in a cyanobacteria suspension. (a-b) Photographs taken of columns of cyanobacteria under two different lighting schemes. When illuminated from above by collimated LEDs, the penetration depth of each wavelength is clearly visualized. (c) The normalized intensity of forward propagating light for five different wavelengths are shown as measured (circles), and as predicted by Cornet's model of 1-dimensional radiation transfer using Schuster's approximation (Cornet et al., 1992a; Cornet et al., 1992b) (solid line) and by the Beer-Lambert equation (dashed line). The radiative transfer model gives a closer approximation to the measured data since it accounts for wavelength dependent scattering by the cells. The measured optical densities for the culture across a 10 mm path length are 1.2, 0.85, 0.75, 0.85, 0.71, 0.49 for 454-nm, 534-nm, 593-nm, 630-nm, 660-nm, and 750-nm light respectively. Based on the radiative transfer model, the attenuation of light gives rise to photic zones of different relative size in each culture scenario for (d) low light and (e) high light. For cultures with initial cell concentration of 0.58 g/L (OD750,10mm = 2.6), dark regions exist in all cases, whereas for initial cell concentrations of 0.04 g/L (OD750,10mm = 0.2), the entire volume is illuminated

Fig. 3. Low-light areal productivity and photon conversion efficiency (PCE). Productivity and efficiency after 1 day of cultivation under 50  $\mu\text{mol photons}/(\text{m}^2 \cdot \text{s})$  light for cultures with initial conditions corresponding to (a) cell concentration = 0.58 g/L (OD750,10mm = 2.6), light path length = 2 cm, (b) cell concentration = 0.58 g/L (OD750,10mm = 2.6), light path length = 6 cm, (c) cell concentration = 0.04 g/L (OD750,10mm = 0.2), light path length = 2 cm, (d) 0.04 g/L cell concentration (OD750,10mm = 0.2), light path length = 6 cm. Error bars represent the standard deviation from three independent trials.

Fig. 4. High-light areal productivity and photon conversion efficiency. Productivity and efficiency after 1 day of cultivation under 2000  $\mu\text{mol photons}/(\text{m}^2 \cdot \text{s})$  light for cultures with initial conditions corresponding to (a) cell concentration = 0.58 g/L (OD750,10mm = 2.6), light path length = 2 cm, (b) cell concentration = 0.58 g/L (OD750,10mm = 2.6), light path length = 6 cm, (c) cell concentration = 0.04 g/L (OD750,10mm = 0.2), light path length = 2 cm, (d) 0.04 g/L cell concentration (OD750,10mm = 0.2), light path length = 6 cm. Error bars represent the standard deviation from three independent trials.

Fig. 5. Accumulated biomass. Graphs showing the total accumulated biomass after 4 days of growth under (a-d) low light and (e-h) high light. Accumulated biomass is reported here in order to communicate the total amount of biomass generated under each different reactor design scenario. When the volume of the shallow reactors is considered the biomass concentrations of the shallow reactors increase much faster than the deep cultures, but this volumetric productivity does not necessarily mean that the shallow reactors produced more total biomass – this can only be compared by looking at the total product generated, as shown here. Error bars represent the standard deviation from three independent trials.

Fig. 6. Pigmentation shift under high light. After four days of growth cells grown under high light with (a) high initial culture density showed a moderate shift in pigmentation and (b) attenuation spectra. (c) Cells exposed to high light with a low initial density showed a much more dramatic shift in pigmentation and (d) attenuation spectra.

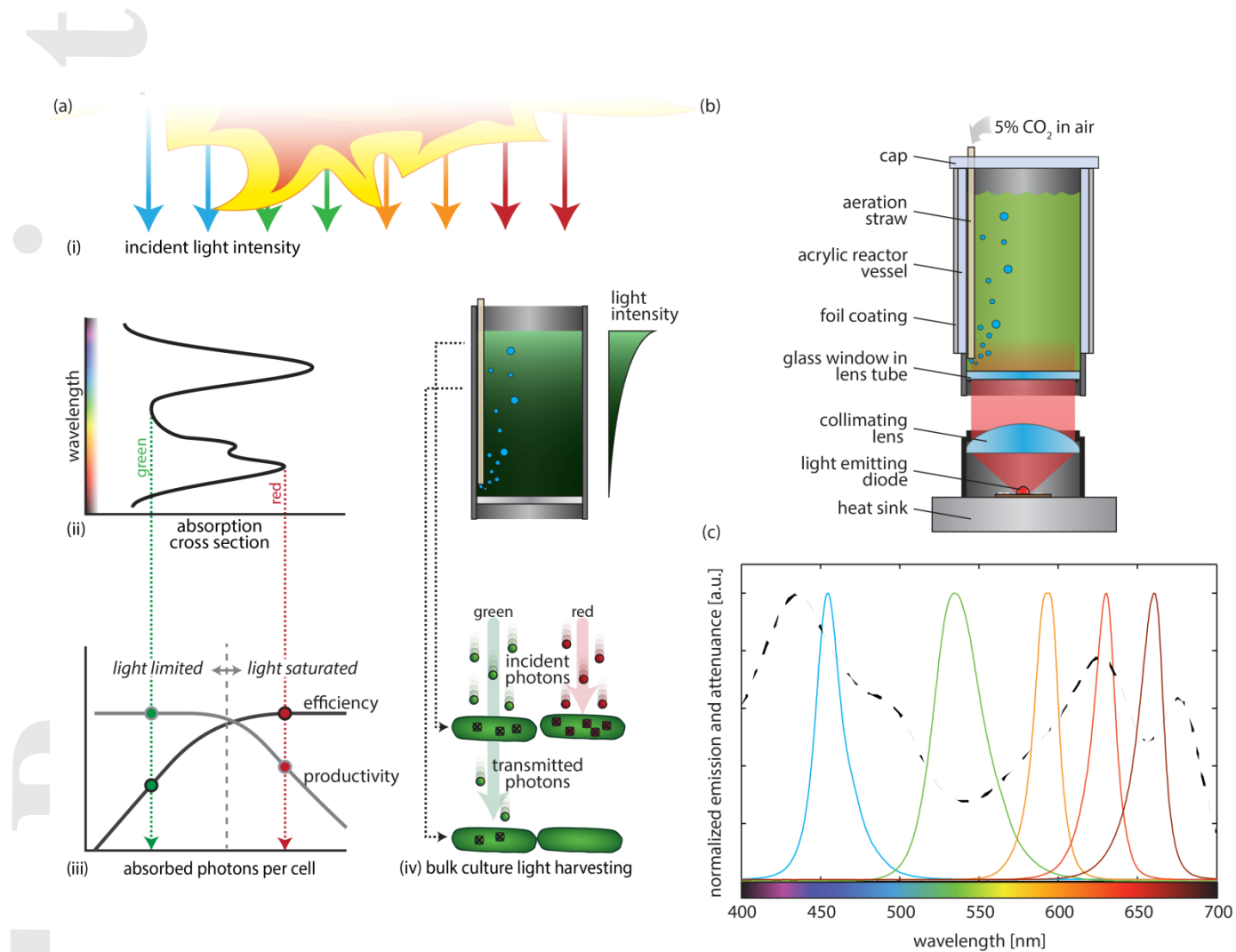


Figure 1

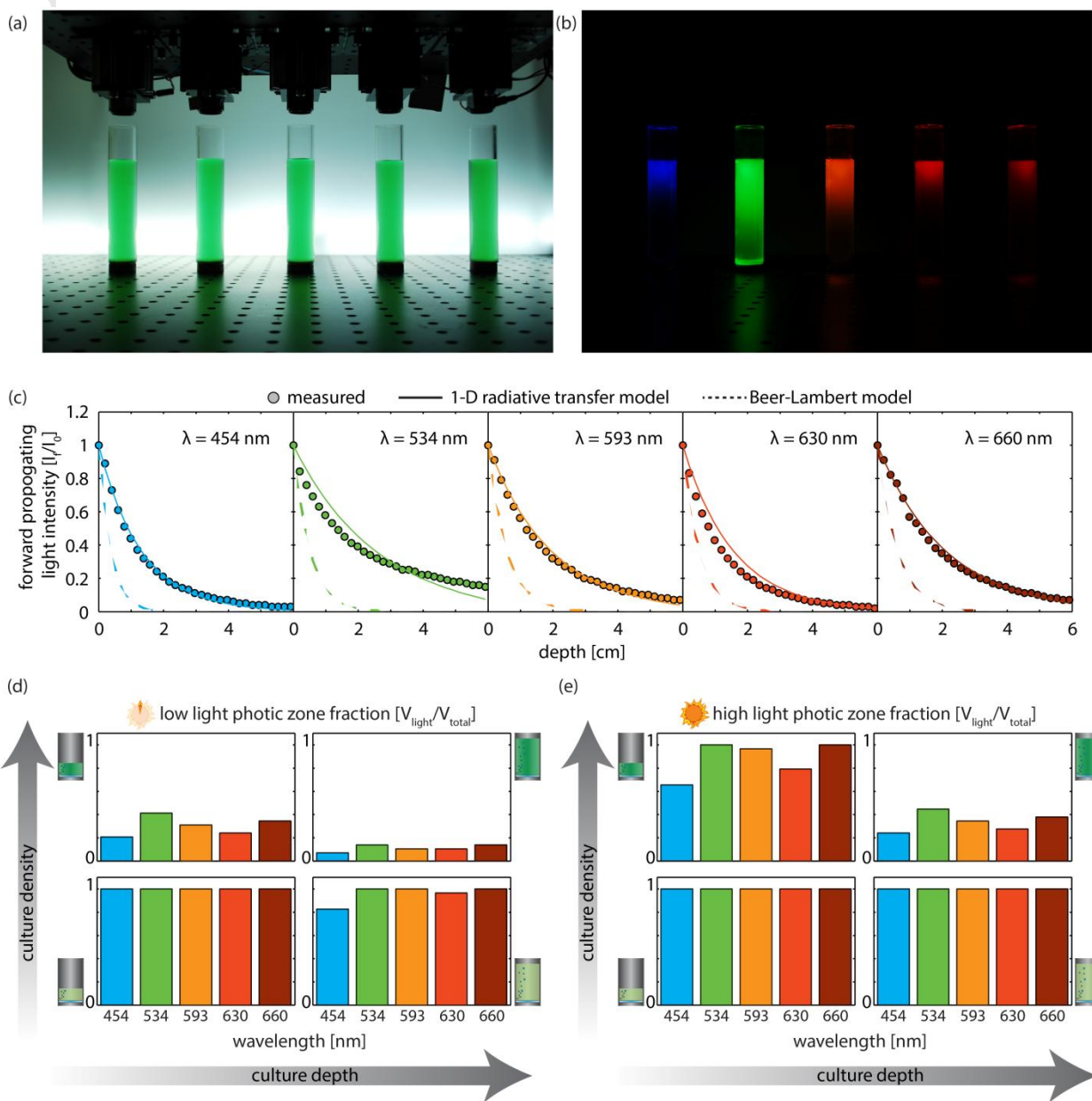


Figure 2

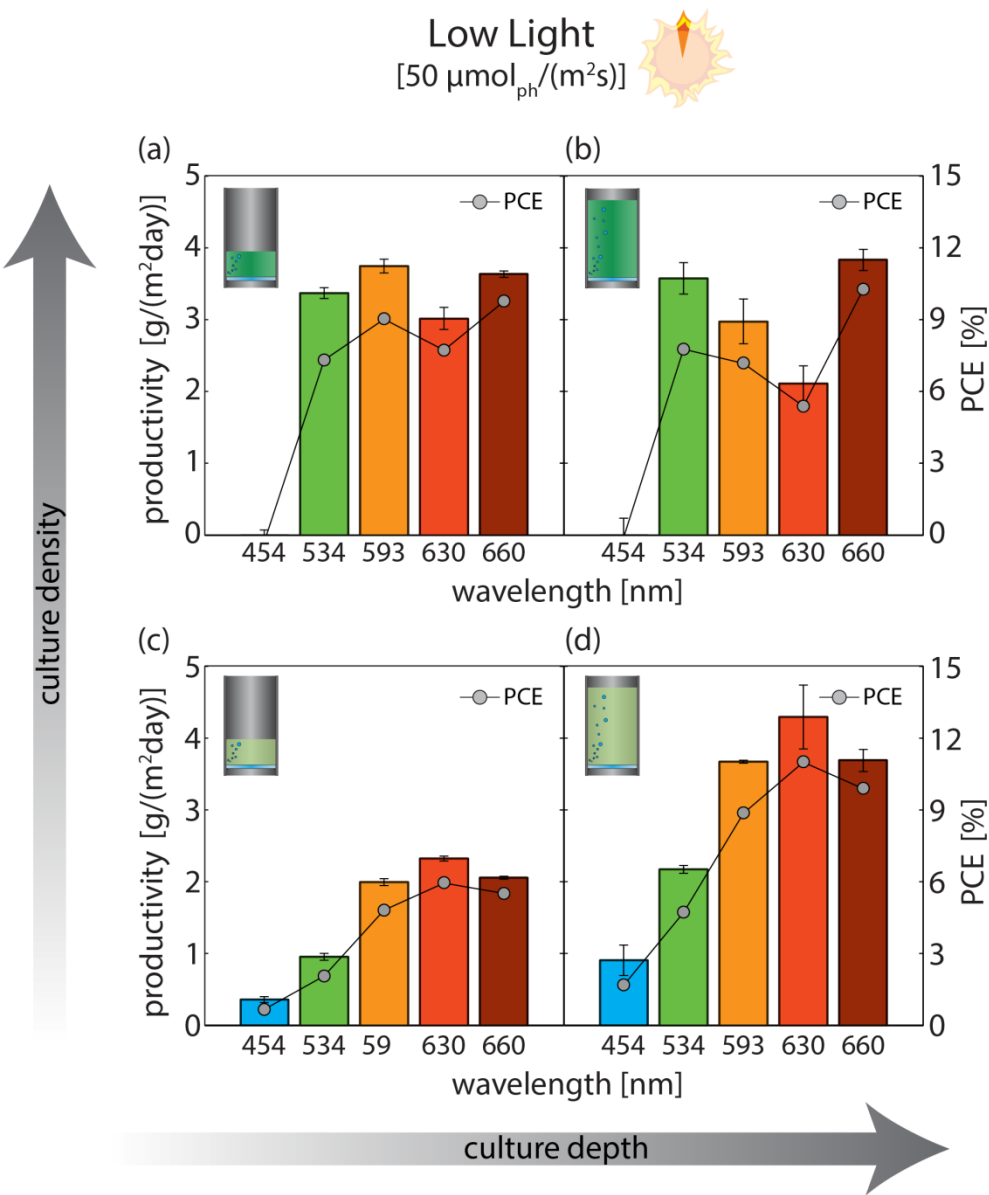


Figure 3



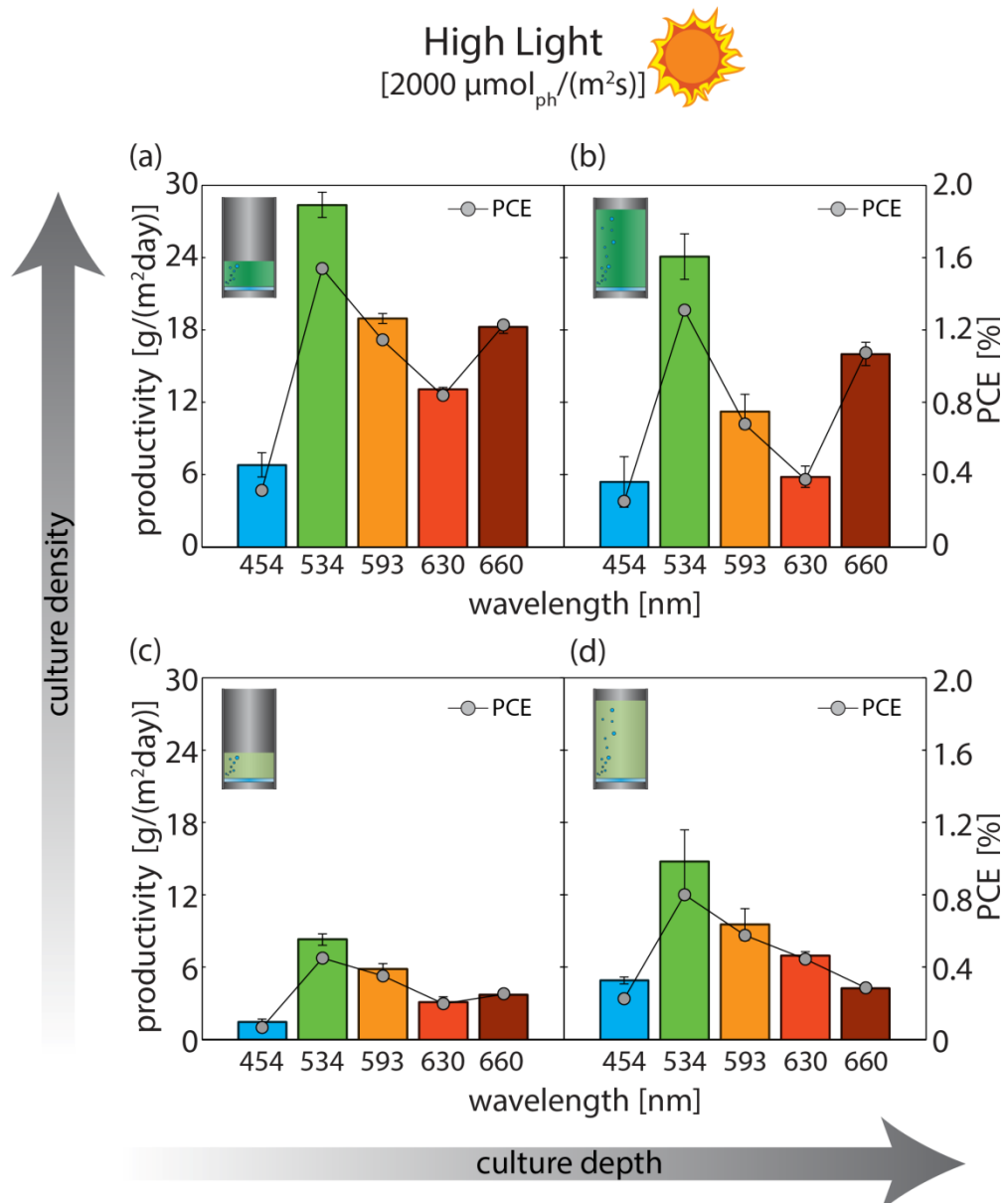


Figure 4

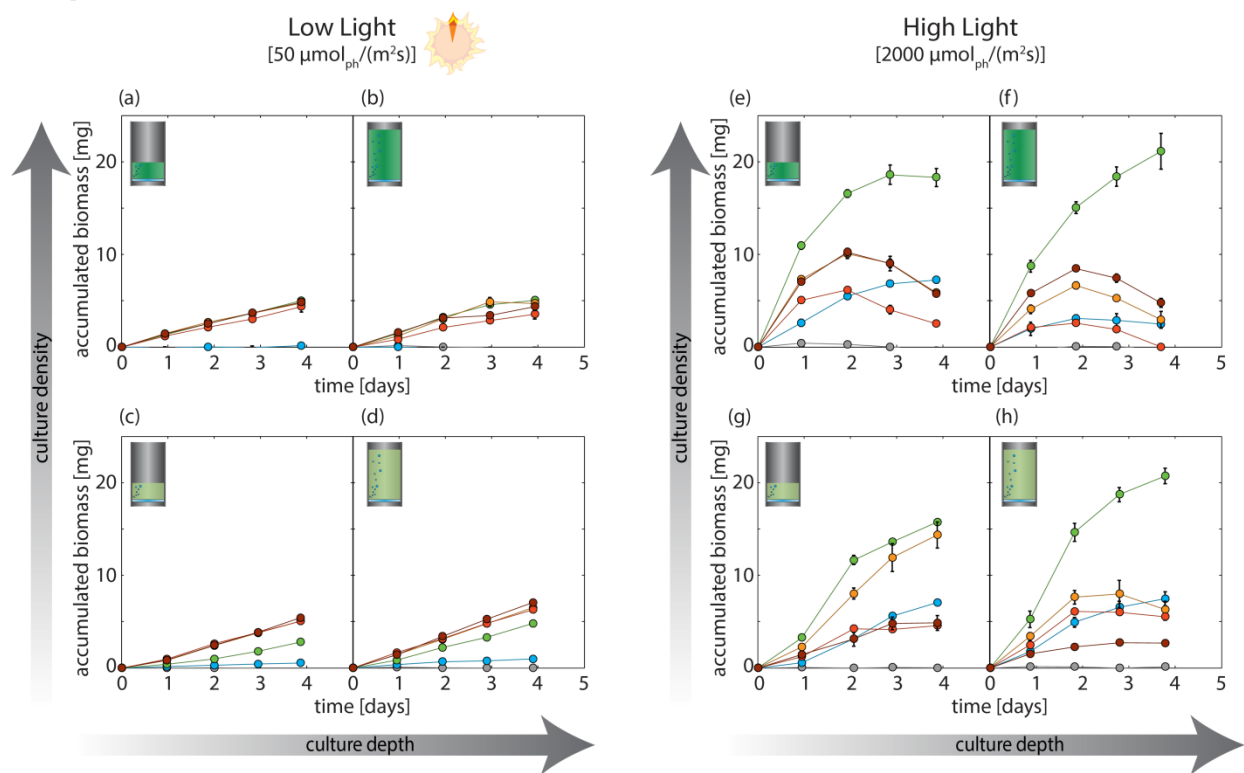


Figure 5

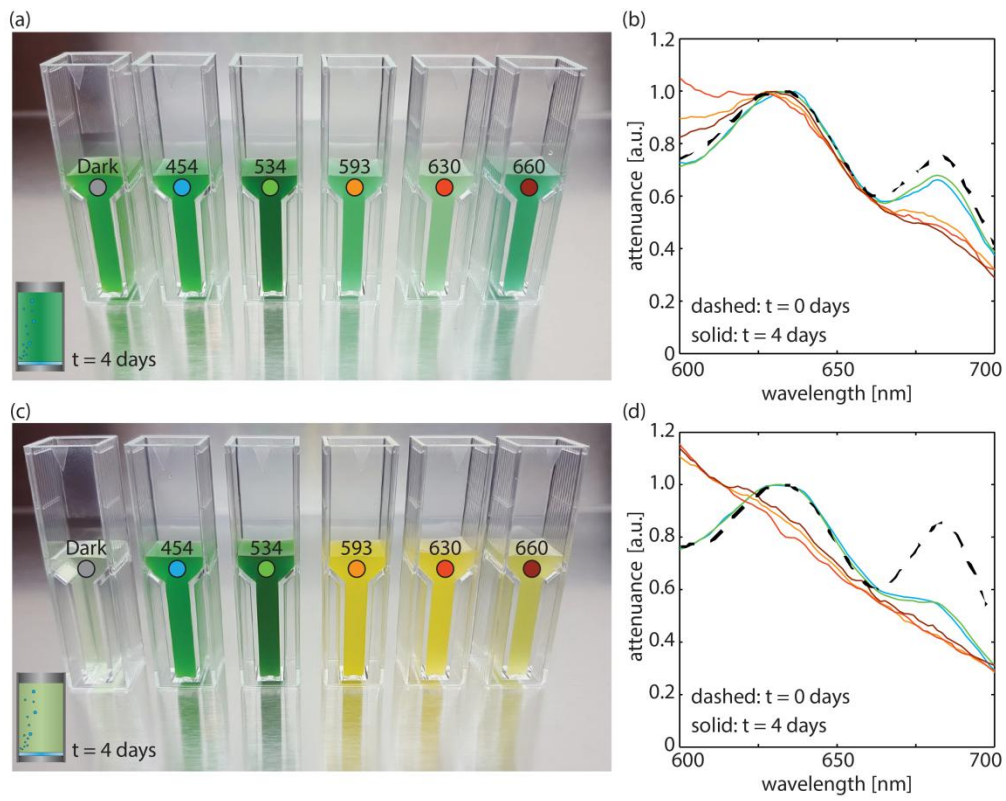


Figure 6